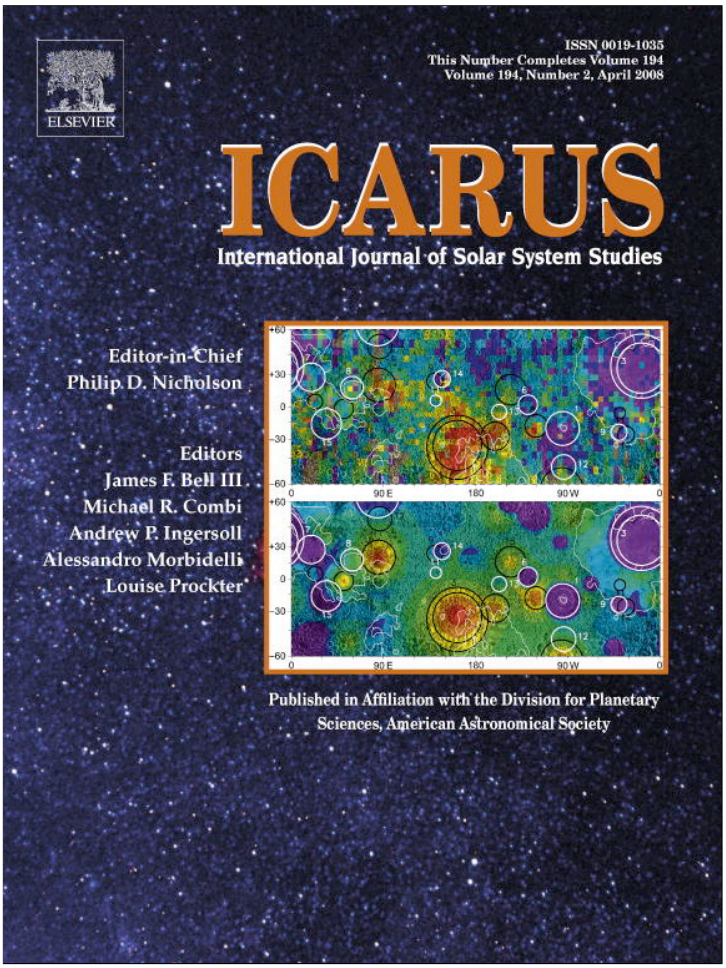

Available online at www.sciencedirect.com
ScienceDirect
Icarus 194 (2008) 690–703
ICARUS
www.elsevier.com/locate/icarus

# Dunes on Titan observed by Cassini Radar

J. Radebaugh [a,*], R.D. Lorenz [b], J.I. Lunine [c], S.D. Wall [d], G. Boubin [c], E. Reffet [e], R.L. Kirk [f], R.M. Lopes [d], E.R. Stofan [g], L. Soderblom [f], M. Allison [h], M. Janssen [d], P. Paillou [i], P. Callahan [d], C. Spencer [a], the Cassini Radar Team

[a] *Department of Geological Sciences, Brigham Young University, Provo, UT 84602, USA*
[b] *Space Department, Planetary Exploration Group, Johns Hopkins University Applied Physics Lab, Laurel, MD 20723, USA*
[c] *Lunar and Planetary Laboratory, University of Arizona, Tucson, AZ 85721, USA*
[d] *Jet Propulsion Laboratory, California Institute of Technology, 4800 Oak Grove Drive, Pasadena, CA 91109-8099, USA*
[e] *LESIA, Observertoire de Paris, 92195 Meudon, France*
[f] *United States Geological Survey Astrogeology Division, Flagstaff, AZ 86001, USA*
[g] *Proxemy Research, Bowie, MD 20715, USA*
[h] *Goddard Institute for Space Studies, 2880 Broadway, New York, NY 10025, USA*
[i] *Observatoire Aquitain des Sciences de l'Univers, UMR 5804, Floirac, France*

Received 22 March 2007; revised 26 September 2007

Available online 21 November 2007

**Abstract**

Thousands of longitudinal dunes have recently been discovered by the Titan Radar Mapper on the surface of Titan. These are found mainly within ±30° of the equator in optically-, near-infrared-, and radar-dark regions, indicating a strong proportion of organics, and cover well over 5% of Titan's surface. Their longitudinal duneform, interactions with topography, and correlation with other aeolian forms indicate a single, dominant wind direction aligned with the dune axis plus lesser, off-axis or seasonally alternating winds. Global compilations of dune orientations reveal the mean wind direction is dominantly eastwards, with regional and local variations where winds are diverted around topographically high features, such as mountain blocks or broad landforms. Global winds may carry sediments from high latitude regions to equatorial regions, where relatively drier conditions prevail, and the particles are reworked into dunes, perhaps on timescales of thousands to tens of thousands of years. On Titan, adequate sediment supply, sufficient wind, and the absence of sediment carriage and trapping by fluids are the dominant factors in the presence of dunes.


*Keywords:* Titan; Satellites, surfaces; Saturn, satellites

## 1. Introduction

The Cassini radar instrument (Titan Radar Mapper) in orbit around Saturn has brought to our awareness many unexpected, Earth-like, geological features on Saturn's largest moon, Titan. River networks (Lorenz et al., 2007; Barnes et al., 2007; Stofan et al., 2006; Elachi et al., 2006; Tomasko et al., 2005) are probably carved by methane and/or ethane, yet are similar in scale and morphology to terrestrial, water-carved channels. Lobate, cryovolcanic flows are likely composed of a water ice mixture, yet are similar in scale and morphology to terrestrial planet basaltic lava flows (Lopes et al., 2007; Barnes et al., 2006; Stofan et al., 2006; Elachi et al., 2005). One of the most surprising of the geological discoveries made thus far for Titan is the presence of thousands of dunes (Elachi et al., 2006; Lorenz et al., 2006). These have interesting variations in behavior and morphology on a local scale, but are largely zonal (W-E, or 90° from N) in orientation, 1–2 km wide, 1–4 km apart, up to 150 m high, and up to more than one hundred kilometers in length (Fig. 1; Lorenz et al., 2006; Elachi et al., 2006; Boubin et al., 2005). They are likely comprised of particulates of primarily organics and some water ice (e.g., Soderblom et al., 2007; see Section 6) and are found mostly near equa-

* Corresponding author. Fax: +1 801 422 0267.
*E-mail address:* jani.radebaugh@byu.edu (J. Radebaugh).

0019-1035/$ – see front matter 
doi:10.1016/j.icarus.2007.10.015

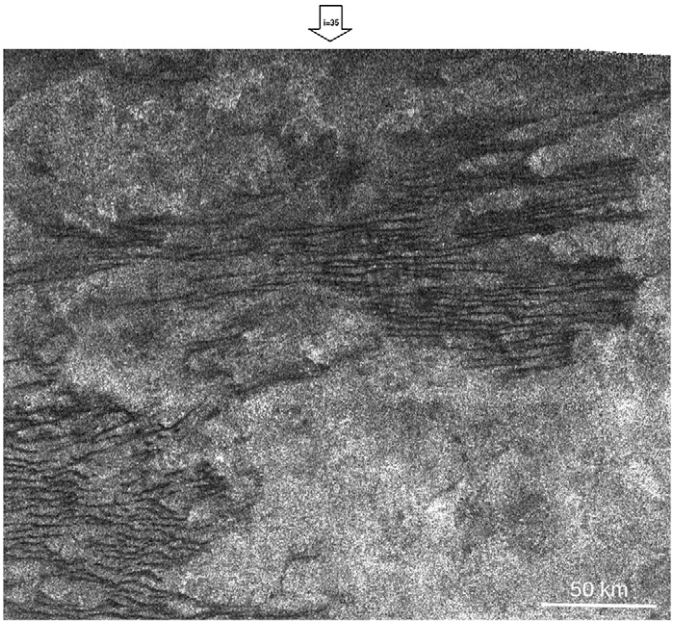


Fig. 1. Dunes seen in the western T3 swath (100° W, 10° N). These dunes exhibit discrete, fine, widely separated, and sinuous longitudinal dune morphologies. Image obtained February 2005, ∼300 m resolution, north is up, arrow indicates direction of radar illumination with incidence angle contained.

torial regions (Lorenz et al., 2006; Radebaugh et al., 2006; Lopes et al., 2006). In the present paper, we follow up on the discovery of dunes on Titan with an assessment of their extent, locations, lengths and orientations, and discuss implications for global and local atmospheric wind patterns as determined from radar observations in the first half of the Cassini tour.

## 2. Correlation of wind and planetary aeolian features as motivation

The mere existence of aeolian features carries the implication that winds can be forceful enough to move surface materials. But the type and orientation of dunes (and aeolian features in general, notably streaks; e.g., Turtle et al., 2007) can be used to infer the net transport direction of material—in essence a weighted vector sum of the long-term wind field. The weighting may be roughly by the cube of wind speed, since transport is highly non-linear (opinions vary as to whether a threshold-and-square law or a cube-law is most appropriate; e.g., Townsend, 1976; McLean et al., 1994). Further, the dune type carries implications about the variability about that vector sum.

Large-scale correlation of wind directions predicted by global circulation models (GCMs) with observed aeolian indicators has been done on Earth (Blumberg and Greeley, 1996) and Mars (e.g., Greeley et al., 1992). In general, good correlations exist, although the resolutions of the models employed in these studies were rather modest (5–10°) and it was noted that sub-grid-scale topography can substantially alter the near-surface wind direction. It may be that for both planets further studies of this type are merited, using the better mesoscale and nested models and much improved remote sensing datasets that have been developed in the last decade.

Saunders et al. (1990) attempted to predict the large-scale patterns of aeolian features based on general properties of the venusian atmospheric circulation. They predicted sand streaks and net sand transport downhill and in the direction of atmospheric super-rotation (on Venus, E-W). While these trends were observed, Dobrovolskis (1993) noted that predicted mean transport would be generally away from the equator, contrary to the wind streaks observed by Magellan. Although introduction of a mean Hadley circulation corrected the direction of predicted winds to be more in agreement with wind streaks, the predicted friction speeds remained inadequate. While these disagreements may be considered in a sense unsatisfactory, they do show how aeolian features can act as an informative constraint on deep atmospheric circulation. Further, it should be noted that while aeolian features (and large dunes in particular) are extremely rare on Venus (Weitz et al., 1994), on Titan their sizes and abundance make prospects much more hopeful for constraining circulation patterns.

Study of dune patterns, and thus winds, is important for improving our fundamental understanding of the tropospheric circulation of Titan and also for planning future exploration missions there. Titan has active precipitation (Tomasko et al., 2005; Porco et al., 2005; Griffith et al., 2006; Tokano et al., 2006) and other similarities to Earth but few other observational constraints, and future missions may use a balloon or other aerial platform and exploit the winds (Tokano and Lorenz, 2006) to cover large areas of the diverse surface.

## 3. Radar observations of dunes

Cassini Radar observations of the morphologies of Titan's dunes are described in this section and the next, first in a broadly introductory manner in chronological order and then in terms of dune interactions with topography. Dunes were first observed by Cassini Radar's 2.17 cm wavelength Synthetic Aperture Radar (SAR) mode in the T3 flyby radar swath (February 2005; 10°–130° W, 0°–20° N; see Elachi et al., 2006) NE of the region Xanadu as thin, radar-dark lines, clumped together in groups of several hundred scattered in patches across the swath (Fig. 1; Table 1). The features, originally termed "cat scratches" before their origin was ascertained, appeared to superpose base materials having more subtle radar variations, and they meandered around or terminated at features of apparently high topography (Fig. 2).

It was determined that these features were longitudinal (linear) dunes, due to their morphologic similarity to longitudinal dunes found on Earth's Namib, Saharan, Arabian, U.S. Southwest, and west-central Australian deserts (Fig. 3; Lorenz et al., 2006), and their similar interaction with surrounding terrain. Dunes have since been observed in all other radar swaths observing regions equatorward of 30° latitude, and up to 55° latitude in isolated cases (Fig. 4). In addition, dunes have been observed in high-resolution areas dark to Cassini ISS (Imaging Science Subsystems, 938 nm; Porco et al., 2005) and spectrally distinct to Cassini VIMS (Visual and Infrared Mapping Spectrometer, in the near-infrared; Soderblom et al., 2007; Barnes et al., in preparation) (Fig. 4).

Table 1
Cassini Radar swaths with dune observations through mid-2007

| Fly-by | Date | Latitude range | Longitude range (W lon) | Swath % w/dunes | Num. measured | Mean length (km) | SD (km) | Mean orientation | SD (°) |
|---|---|---|---|---|---|---|---|---|---|
| T3 | 02/15/2005 | 0°–20° N | 10°–130° | 40 | 2350 | 16 | 10 | 88° | 24 |
| T8 | 10/28/2005 | 5°–20° S | 190°–320° | 70 | 3294 | 38 | 21 | 82° | 14 |
| T13 | 04/30/2006 | 5°–20° S | 70°–170° | 20 | 1082 | 31 | 18 | 109° | 17 |
| T16 | 07/22/2006 | 20°–80° N | 320°–180° | 5 | 168 | 51 | 24 | 84° | 14 |
| T17 | 09/07/2006 | 5°–10° N | 40°–80° | 90 | 1027 | 33 | 17 | 82° | 14 |
| T19 | 10/09/2006 | 0°–85° N | 340°–150° | 10 | 455 | 48 | 34 | 82° | 14 |
| T21 | 12/12/2006 | 30° S–50° N | 180°–300° | 20 | n.y.a. | n.y.a. | | n.y.a. | |
| T23 | 01/13/2007 | 40° S–60° N | 330°–100° | 15 | n.y.a. | n.y.a. | | n.y.a. | |
| T25 | 02/22/2007 | 30° S–85° N | 340°–60° | 15 | n.y.a. | n.y.a. | | n.y.a. | |
| T28 | 04/10/2007 | 20° S–80° N | 340°–40° | 10 | n.y.a. | n.y.a. | | n.y.a. | |
| T29 | 04/26/2007 | 0°–85° N | 320°–40° | 5 | n.y.a. | n.y.a. | | n.y.a. | |

*Notes*. Comparative morphologic analyses have been done for all swaths listed (n.y.a. = specific measurements not yet available). Lengths shown terminate at branches (see text). See Fig. 4 for swath locations.

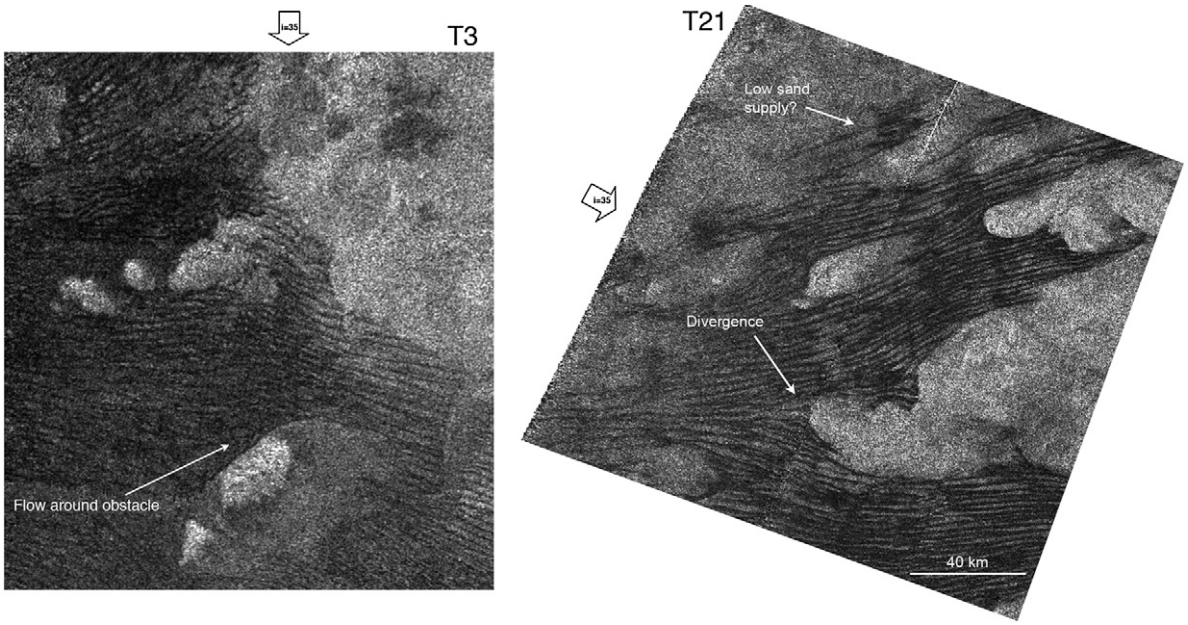


Fig. 2. Dunes from the T3 (∼20° W and 5° N) and T21 (∼20° N, 280° W) swaths. These features are affected by topography. Dunes in the eastern T3 swath change orientation from W-E to NW-SE and to SW-NE at the western margin of the ejecta blanket of Sinlap crater, seen on the east side of the image. Isolated, radar-bright features are radar illuminated peaks with erosional blankets that, along with dunes, indicate a wind direction of E-SE. Dunes in the T21 image divert to the north and some to the south of the western margins of topographically high obstacles. Images obtained February 2005 and December 2006, ∼300 m resolution, north is up, arrows indicate direction of radar illumination for each with incidence angle contained.

In the T8 observation (October 2005; 190°–320° W, 5°–10° S) dunes were found in the radar- and optically-dark region Belet in the form of massive dune regions termed “sand seas” (Fig. 5; Lorenz et al., 2006; Lunine et al., 2008). Dunes in sand seas are closely spaced, are highly linear in form, and often have radar-dark (though not as dark as the dunes) interdune material. Radar backscatter reflection from Cassini-facing, or uprange, surfaces was observed in Belet, indicating the radar-dark features are topographically high compared with their surroundings, and further confirming their classification as dunes.

Identification of features on Titan can be highly dependent on radar look direction (see Paganelli et al., 2006). We compared overlapping observations of a dune region near 290° W longitude obtained from different look directions to address the question of whether dune identification is dependent on radar look direction. Given that nearly every dune that is visible in one image is visible in the other obtained at nearly 70° azimuth from the first (Fig. 6), we conclude that look direction is not as important for dune identification as for other features. Thus dunes are likely compositionally different from surrounding and underlying materials (or materials in the dunes absorb radar better due to their particulate nature). One dune feature stands out prominently in one image in Fig. 6, however, and not the other. Radar-bright lineations can be seen on dune faces oriented perpendicular to the direction of radar illumination, due to reflection off a sloping surface (Fig. 6), similar to the reflections seen in the Belet region described above.

(a)

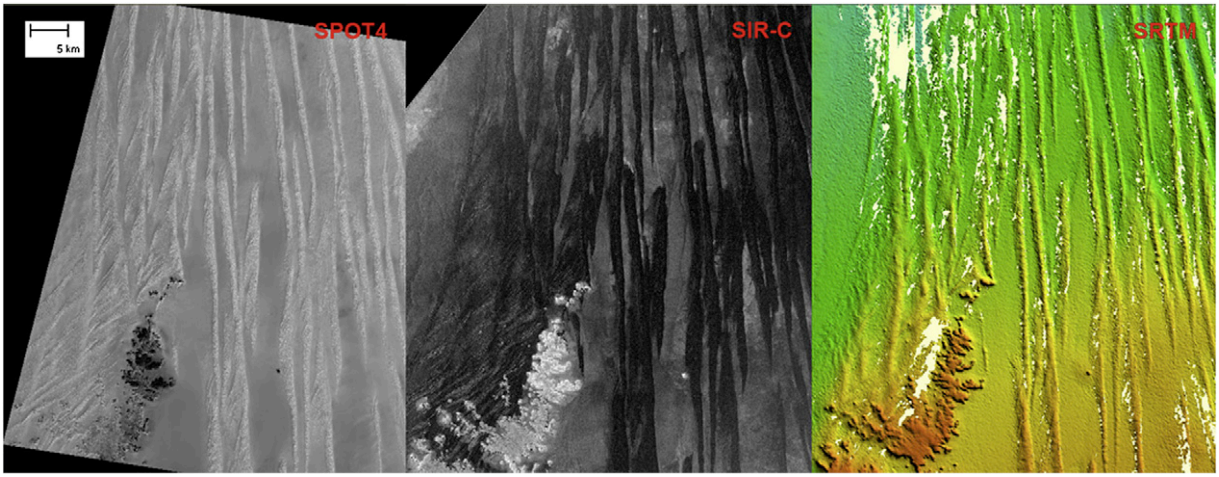


(b)

Fig. 3. (a) Hand held image taken by R. Lorenz of longitudinal dunes near Moenkopi, NE Arizona. Although many of the dunes are stabilized by vegetation, their longitudinal form is evident. The dunes are affected by topographical obstacles, as is seen on Titan. (b) SPOT4 (visible)/SIR-C (C-band SAR)/SRTM (topography) scene of a region of the Great Sand Sea in southwestern Egypt. The Great Sand Sea spans 650 km between Siwa Oasis in the north and the Gilf Kebir plateau in the south. Its average width is about 300 km from the Libyan border to the west and Farafra Oasis depression to the east. The dune axes trend north–south, parallel with the prevailing wind direction. The imaged region is located around (24° 30″ N, 25° 55″ E) and covers approximately 55 by 70 km. North is up. Linear dunes are deviated by a small plateau located in the lower left part of the image (mean altitude 800 m). Dune height is around 70 m and mean dune separation is about 1.5 km. SPOT4/SIR-C/SRTM images courtesy of NASA.

## 4. Dune interactions with topography

Dunes often show they have been morphologically controlled by features having bright/dark pairings indicative of high topography termed "mountains" (Figs. 2 and 5; Radebaugh et al., 2007). These mountains are radar-bright, due to slope illumination (with paired dark pixels due to shadowing of downrange slopes), to the compositional or structural nature of the bedrock, and to the roughness at 2.17 cm of the erosional blankets surrounding the peaks. Mountains in dune regions can approach 2 km in height above their surrounding base materials, which gradually slope down to the regional base level (Radebaugh et al., 2007). Moderately radar-bright aureoles of extent several to tens of kilometers often extend from the mountains roughly to the east, aligned with the dunes in that region (Fig. 2). These have blunt margins on the west sides of the mountains, and they gradually merge into the background materials to the east. They are interpreted as materials that have been eroded from the mountains, likely by methane rainfall, and redeposited by eastward-flowing winds (Fig. 2; Barnes et al., 2007; Radebaugh et al., 2007). These preferentially oriented aureoles are radar-bright, probably as a result of compositional differences from underlying materials rather than from roughness at 2.17 cm. This is because Titan's winds do not regularly transport materials of this size (Lorenz et al., 2006) and these observations are consistent with infrared (ISS and VIMS) observations of the same areas. Dunes at the western margins of mountains are shorter and are oriented slightly north and south of the original Eastward direction. Dunes appear to curve around mountain margins, becoming parallel to the typical dune direction for the area away from these margins. This is seen in many regions, such as near Sinlap crater, which was observed in the T3 swath (∼15° W, 10° N) (Fig. 2). The presence of multiple obstacles can lead to a broad sinuosity of the dunes on a wavelength scale similar to the spacing of the obstacles. This is observed in dunes of the Fensal sand sea NE of Xanadu,

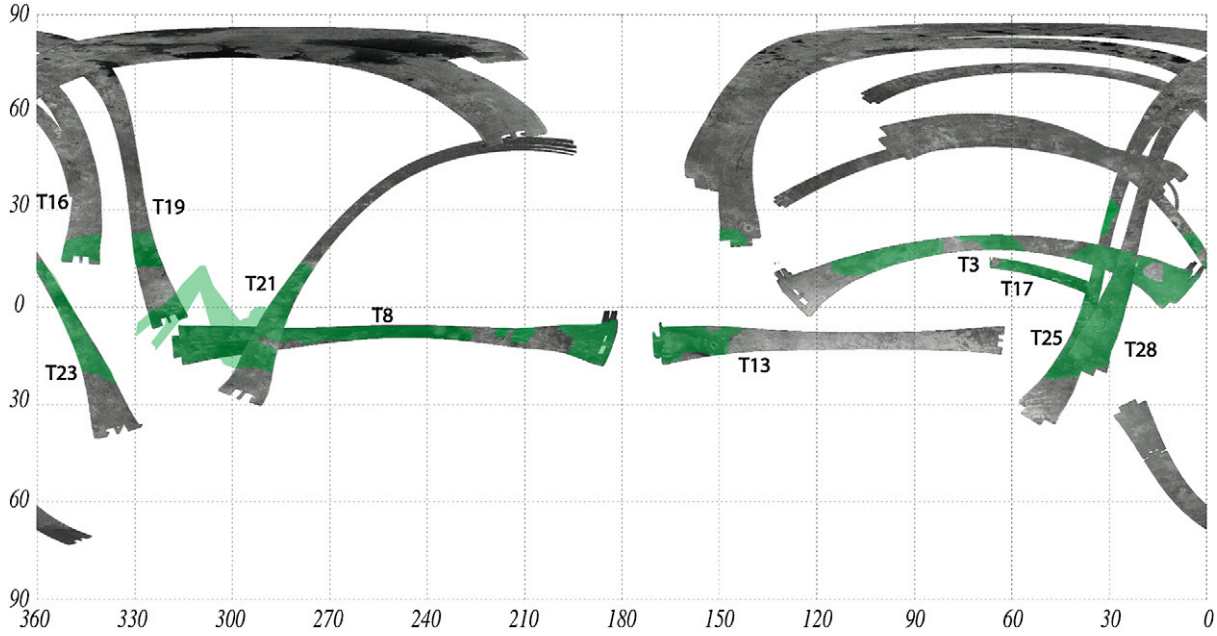


Fig. 4. Plot of dune coverage on Titan as seen in Cassini Radar swaths. All regions on Titan containing a high proportion of dunes as seen in SAR swaths (Ta through T28) are outlined in dark green. Swaths are delineated by flyby number and are labeled close to the major dune areas. Dune-populous areas occur at Titan's equatorial regions.

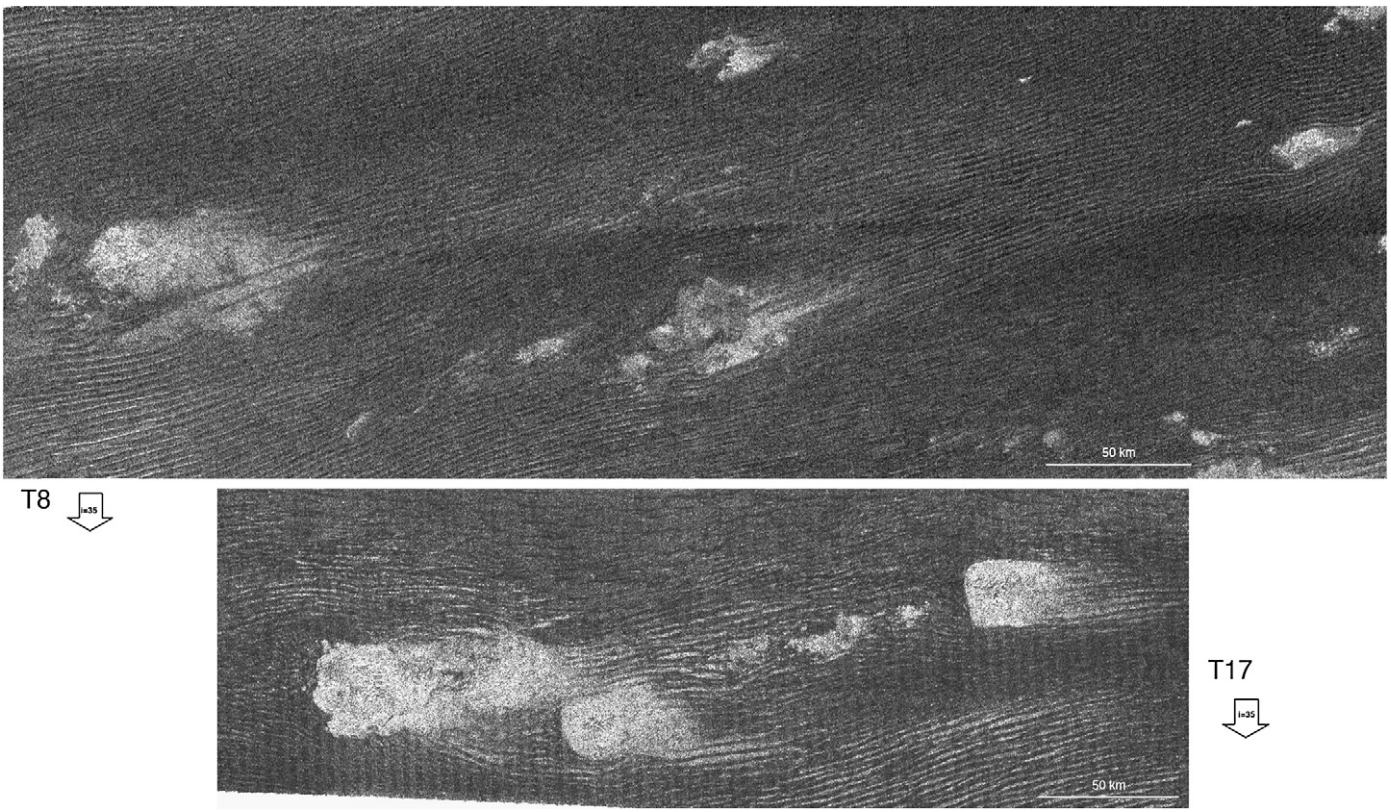


Fig. 5. Dunes in the T8 Belet sand sea (top, ~260° W, 5° S) and the T17 Fensal sand sea (bottom, ~50° W, 10° N). Both regions are effectively covered in dunes that are closely spaced and highly parallel. Dunes divert around mountains and other topographic features, and they create a broadly sinuous pattern in the T17 image. Radar-bright, underlying substrate can be seen between some dunes, in particular, close to topographic obstacles in the T17 region. In the lower left corner of the T8 image, bright lineations associated with the dunes are radar backscatter returns indicating steep, uprange faces. Images obtained October 2005 and September 2006, ~300 m resolution, north is up, arrows indicate direction of radar illumination for each with incidence angle contained.

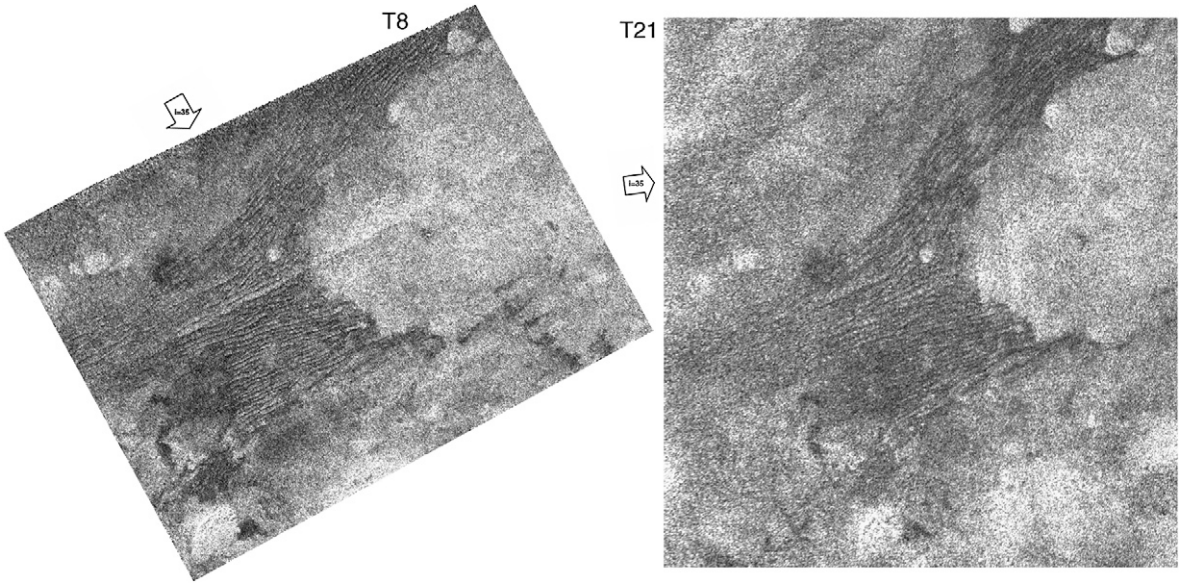


Fig. 6. Images of the same region at ∼10° S, 280° W, obtained October 2005 (T8) and December 2006 (T21). These reveal that dune detection is not strongly dependent on radar viewing angle, as these were obtained with a 70° separation of radar azimuth. Most individual dunes are visible in both images; however, some features differ between images. Radar reflection off of dune faces is only evident when radar azimuth is perpendicular to the dune long axis (T8 image, left), and further confirms that dunes are in fact positive-relief features. ∼300 m resolution, north is up, arrows indicate direction of radar illumination for each with incidence angle contained.

obtained in the T17 swath (September 2006; 40°–70° W, 5°–10° N; Fig. 5).

Dunes on the western and northern margins of the Belet sand sea, seen in the T21 observation (December 2006; 20° S–30° N, 260°–300° W) are similar in morphology to the short, widely-spaced dunes of the T3 region. They are distinct from surroundings, divert around topography and terminate at regions that may have a sufficiently high slope to preclude dune progression (Fig. 2). This is also true for dunes east of Sinlap crater in the T23 swath (January 2007; 20° N–25° S, 340°–10° W) that wrap around topographically high, bright features and overlap lower features. That dunes do not climb up on topographic obstacles is a limitation on the slope of the feature. For example, Cooke et al. (1993) states that an obstacle must have a steep upwind slope (30°–50°) to prohibit dunes from climbing (see also Bourke et al., 2004). However, most measurable mountain peaks on Titan have slopes of ∼10° (Radebaugh et al., 2007) with surrounding blankets much less steep, so further research must be done in this area.

The radar- and optically-bright region Xanadu, found at Titan's equatorial leading hemisphere (90° W–150° W), may be slightly elevated above surrounding terrains. Evidence for this includes observations of dunes just west of Xanadu, imaged during the T13 flyby (April 2006; 5°–15° S, 150°–170° W). These are closely spaced, with radar-dark interdune materials, similar to dunes in the other sand seas, Fensal and Belet. These dunes show marked evidence of diversion around Xanadu, as most dunes are oriented SE just west of the Xanadu margin.

## 5. Dune sizes

Using 1-D radarclinometry across the radar-bright (uprange) and paired dark surfaces (indicating radar shadowing on the downrange surface) of dunes in the Belet sand sea, slopes of ∼10° and related heights of 100–150 m were determined (Lorenz et al., 2006; Kirk et al., 2005). These are similar to the slopes and heights of Namib longitudinal (linear) dunes (Lorenz et al., 2006; Bagnold, 1942; Lancaster, 1982) and to sizes of features seen by VIMS and ISS (Barnes et al., in preparation; Turtle et al., 2007). In addition, echo widths from radar altimetry compared to waveform simulations over dunes correspond to heights of 100–200 m and spacings $\gtrsim$10 times the height (Callahan et al., 2006), in good agreement with SAR observations and radarclinometry measurements.

We measured widths, lengths, separations, and orientations of all dunes on Titan observed through the T19 flyby (October 2006). All measurements were made on features in oblique cylindrical BIDR images (256 pixels/degree, range and azimuth resolution ∼300 m) obtained when Cassini RADAR was in SAR imaging mode. The USGS image processing program ISIS was used to obtain start/end latitude/longitude positions and lengths of features, from which were derived orientations clockwise Titan polar north. A dune is considered to have a W-E (90° from north) orientation if a line parallel to its long axis is oriented parallel to Titan's lines of equal latitude. 2315 dunes measured from the T3 swath had a mean width (width being the short-distance extent of dark material) of 1 km, while 1255 had a mean dune spacing (crest-to-crest distance) of 3 km. These mean widths and spacings are similar to those of longitudinal dunes in the Saharan and Namibian deserts (Lancaster, 1989). Comparably extensive measurements of dune widths and spacings have not yet been systematically made in other regions; however, spot checks give typical widths of 1–2 km and spacings of 1–4 km.

Small-scale (<200–300 km on a side) dune fields with definite margins have dunes with the most discrete appearance, and

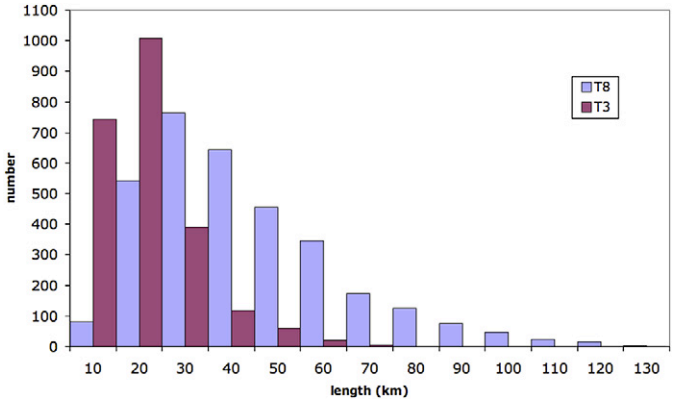


Fig. 7. Dune lengths for the regions of sparse dune field populations (T3) and for sand seas (T8). Dunes in the sand seas region are longer than those restricted by sand supply and obstacles.

thus the most easily quantifiable dune lengths. 2350 dunes measured in the T3 swath have lengths ranging from 1 to 79 km and a mean length of 16 km (Fig. 7; Table 1).

Lengths of dunes in sand seas are quantified differently than in the smaller dune fields. The Belet sand sea stretches nearly 2000 km, and there are dunes across its length, but dune forms in this area are more complex and make beginnings and endings more difficult to determine. We chose to stop measuring a dune if it (1) could no longer be seen, (2) branched (for example in Y-junctions), or (3) changed direction. These criteria may have led us to systematically underestimate the length of dunes, so the absolute length values should be regarded with some reservation. Any measurement bias should be similar in all areas, however, so that the results will still be useful for comparing dune lengths across different regions. Dunes in the Belet sand seas, for example, are longer on average than those in the T3 region, where we interpret topographical features and smaller sand supply preclude the formation of long dunes (Fig. 7; Table 1). Terrestrial sand seas often extend for hundreds of kilometers (McKee, 1982; Lancaster, 1982) and individual dunes with multiple branches have been measured to extend well over 100 km (Lancaster, 1995). Future surveys of Titan's dunes ignoring branching as length delineators can be compared with these terrestrial surveys, and will undoubtedly produce a substantial number of dunes $>100$ km in length.

## 6. Dune type and composition

Longitudinal dunes are classified as such on Earth based on their length (usually more than 20 km), straightness, parallelism, regular spacing, and ratio of high dune to interdune areas (Lancaster, 1982). There are many morphological variations on this general form. On Titan, dunes are organized into two major categories, described here and above as dune fields and sand seas. Dune fields, such as those found in isolated patches or on the margins of sand seas, are small (from several to a few tens of kilometers long), highly discrete, and have a dune spacing greater than the global mean of 2 km. In some regions, these dunes are highly sinuous on a short-wavelength scale (Fig. 1). Sometimes the dune ends diverge, further increasing their local separation, or seem to gradually dwindle out. These dunes either form in regions of relatively low sand supply, are restricted by topographic constraints, such as elevated landforms, or are at a different evolutionary stage than those in the sand seas. These observations are consistent with the behavior of dunes on Earth so constrained (Fitzsimmons, 2006), which lends support to this interpretation of smaller sand supply and topographic restrictions altering dune morphologies.

Dunes in Titan's sand seas have a dune spacing of ~1 km, less than the global mean of 2 km, and often have radar-dark interdune material, indicating a high amount of sediment in those regions. These dunes are very straight for many tens to hundreds of kilometers, and are highly parallel. Because of their small dune spacing, there are a greater number of branches in a given area than in the dune fields. Despite these variations in morphologies in the two major dune region types, the vast majority of dunes on Titan are still classified as longitudinal. In fact, there are very few dune fields on Titan observable at radar resolution (~300 m/pixel) that are not longitudinal in type. In a couple of isolated regions near topography, dunes are more closely spaced and sinuous and have orientations perpendicular to the regional trend, typical of transverse dunes (illustrated in Lorenz et al., 2006). A couple of other regions have two clear longitudinal dune trends at angles separated by less than 60°, overprinted on one another (Fig. 8). These regions are relatively small ($<100 \times 100$ km) and may be associated with the interaction of winds with topography or with a regional or seasonal shift in general wind direction.

Material properties on Titan are not yet well known. Regions determined to be water ice-rich and separately aerosol-rich (perhaps tholin dust) by Cassini VIMS do not have an obvious correlation with regions that are near-infrared (ISS) and radar-bright across Titan's surface (Soderblom et al., 2007), indicating surface chemistry processes are complicated and not easily delineated geomorphologically. However, perhaps the best correlation across instruments in terms of Titan's surface composition may occur in the dunes. Dunes are dark in radar and near-infrared images (ISS and VIMS) (Soderblom et al., 2007; Porco et al., 2005; Barnes et al., in preparation) and correlate with the VIMS dark brown units, which are inferred to be water ice-poor (Soderblom et al., 2007). Radar radiometry measurements of dune regions suggest the measured dielectric constant is consistent not with water ice but with fine-textured organics (Paganelli et al., 2007a, 2007b). Very low volume scattering is seen in the dunes, which could result from signal return from smooth surfaces with homogeneous, highly absorbing, fine-grained particles of solid organics (Paganelli et al., 2007a, 2007b). Given the dune morphology and known atmospheric density at Titan's surface, we estimate the saltating particles to be 100–300 μm in size (Lorenz et al., 2006). Aerosols reworked into hydrocarbon and/or nitrile solids may precipitate from the atmosphere in solid form (think snow; Soderblom et al., 2007). These may combine with products created by methane rainfall and erosion of water–ice bedrock to be deposited in low areas. Persistent winds in Titan's dense

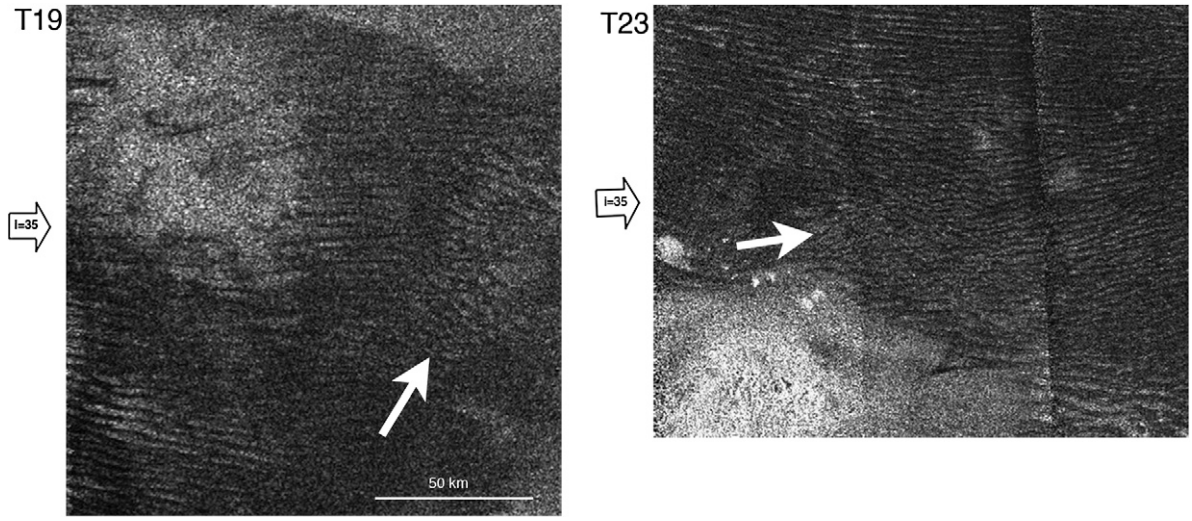


Fig. 8. Dunes from the T19 (October 2006, 10° N, 320° W) and T23 (January 2007, 0°, 350° W) swaths. These regions (located by white arrows) show two dominant dune long axis orientations separated by approximately 60°, indicating a local change in wind pattern. Images ~300 m resolution, north is up, arrows indicate direction of radar illumination for each with incidence angle contained.

atmosphere then entrain the particulate deposits and organize them into longitudinal dunes.

## 7. Dune orientations and wind direction

Longitudinal dunes form in Earth's deserts under several major and widely different wind regimes. They can be found in wide unimodal (winds from one main directional sector), bidirectional (winds from two distinct directions) and even complex (more than two modes) wind regimes (Fryberger and Dean, 1979). Beyond minor characteristics, such as crestline sharpness and meander (e.g., Tsoar, 1983), which are not visible at Cassini Radar resolutions, these different wind regimes do not provide profound clues to their presence through dune morphologies. Other clues must be analyzed with dune orientation to provide evidence of wind direction. The prevailing wind hypothesis of longitudinal dune formation, based on conditions of wide unimodal winds, involves transportation of sediments along the dune axis. Thus winds prevail in a direction parallel to the long axis of the dunes with minor off-axis components (e.g., Blandford, 1877; Folk, 1971; Fryberger and Dean, 1979; Lancaster, 1995). The off-axis components act to "shepherd" the dunes into their linear forms and to remove the sands from in between the dunes, exposing the underlying bedrock. The long axes of most dunes on Titan are regionally parallel to the thin, radar- and near-IR-bright blankets that flank the eastern sides of topographic features, thought to be blankets of eroded material blown downwind. Also, many dunes curve around the western margins of obstacles and resume their original orientations on the eastern margins, similar in many ways to fluid flow around obstacles and islands in a stream bed. Finally, winds measured by the Huygens probe, which landed near the equator east of the Belet sand sea, were toward the east near the surface (Tomasko et al., 2005). For these reasons, the prevailing wind hypothesis for dune formation is appealing for Titan. Because dunes are oriented mostly W-E (Figs. 1, 2, 5, 6, and see below), this means that winds on Titan between ±30° latitude are dominantly eastward, related to zonal winds of similar direction (Bird et al., 2005), but with minor, fluctuating tidal winds (Lorenz et al., 2006).

However, there are also aspects of the two-wind, or resultant, model of dune formation (e.g., Tsoar, 1983; Lancaster, 1995; Rubin and Ikeda, 1990), which is based on conditions of bidirectional winds, that have merit for Titan. This wind regime exists in the Namib sand sea in SW Africa, where there are many morphological analogues for Titan. Most of the year, winds blow from the SW, but in the winter they change dramatically to come from the NE (Lancaster, 1980; McKee, 1982). This situation causes the formation of longitudinal dune forms on the scale of those on Titan, it leads to the divergence of dunes around topographic obstacles, and it means yearly averaged sand transport rates are low, leading to an overall accumulation of sand in the Namib sand sea region (Wilson, 1971; Fryberger and Ahlbrandt, 1979). In addition, it could help explain why particles have accumulated in Titan's sand sea regions. A dramatic, seasonal shift in wind direction, similar to what occurs in the Namib sand sea, could lead to net deposition of sand in the sand sea regions. Another possibility is that sand transport is affected by large topographic features, such as Xanadu, which rests east of Belet and related sand seas and west of Fensal, as has occurred on Earth (e.g., Mainguet and Callot, 1978; Bowen and Lindley, 1977). This bidirectional wind condition would also help resolve the current paradox between observations of dune morphologies and tidal wind models that call for westward wind flow (Tokano and Neubauer, 2005).

Based on the discussion above, we assume that dune orientations, in conjunction with wind streaks and other patterns listed above, can be used to provide constraints on local, regional, and global mean wind directions. We report orientations for 8376 dunes measured in the T3, T8, T13, T16, T17, and T19 swaths (Table 1; Fig. 9). Detailed distributions of dune orientations for each swath taken as a whole are outlined. The swaths are long and narrow compared to the more equant areas that one might

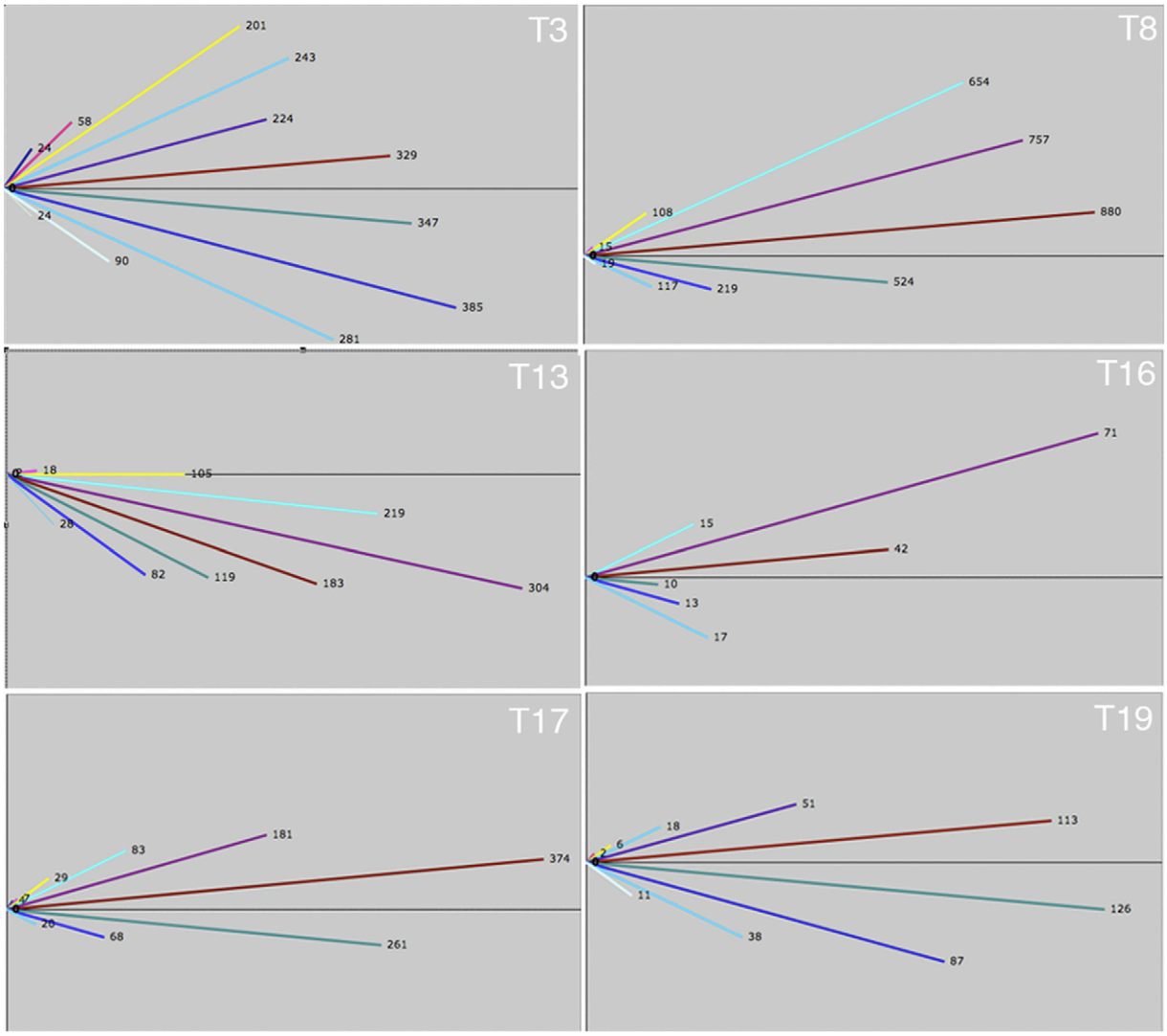


Fig. 9. Orientations of all dunes reported by swaths as rose diagrams, with line lengths corresponding to numbers of dunes found at that orientation. T3 covers the region north of Xanadu and has two impact craters and a number of mountains, T8 is within the Belet sand sea, T13 covers the sand sea west of Xanadu, T17 is in the Fensal sand sea north east of Xanadu, and T19 is at the equator, west of Belet (see Fig. 4 for swath locations).

choose to sample different terrains if not limited by the image coverage, but dunes measured within a single swath are typically found within only one or two major regions, and thus statistics from them can be considered regional in scope (see Fig. 9 caption). Both across swaths and within smaller regions, dune orientations are roughly W-E (90° from N). This is likely a direct reflection of the long-term mean wind direction. Note (Fig. 9) that there is not much variation from the mean orientation of 88° in dunes from the T8 swath (SD 14°), where the relatively uniform Belet sand sea (Fig. 4; 230°–290° W, 5° S) dominates dune trends, while there is considerable scatter from the mean orientation of 70° (SD 24° in dunes from the T3 swath (see Fig. 4), where there are more isolated dune patches working their way around topography.

The T3 swath also covers the area just north of the mountainous region Xanadu, and T3 dunes show a broad trend of arcing around Xanadu. Dunes at the west end of T3 (100°–130° W, 0°–5° N), have a mean orientation of 86° (Boubin et al., 2005) while dunes found in the middle of the T3 region (50°–80° W) have a mean orientation of 77°. Those dunes found on the east end of the T3 swath (10°–30° W) have a range of orientations related to divergence around the 80 km diameter impact crater Sinlap (Fig. 2). Dunes south of Sinlap have a mean orientation of 120°. These data reveal that dunes have been diverted by topographic features on a local and a regional scale.

The T13 dunes, found on the west margin of Xanadu (see Fig. 4), have a mean orientation of 109° (SD 17°). Again, the winds in this region demonstrate the appearance of diverting around Xanadu in the form of a southward deviation of dunes from the typical W-E.

To observe changes in wind patterns on a more local scale, dunes were analyzed in 5° × 5° latitude–longitude boxes across Titan. Several interesting patterns are evident (Fig. 10). First, dunes in the broad, relatively uninterrupted Belet sand sea just below the equator (230°–290° W, 5° S) may reveal the most "typical" wind pattern for equatorial Titan, almost exactly eastward, with a slight equatorward trend (to the N). This equatorward trend is also seen in the T17 swath (40°–70° W, 5°–10° N)

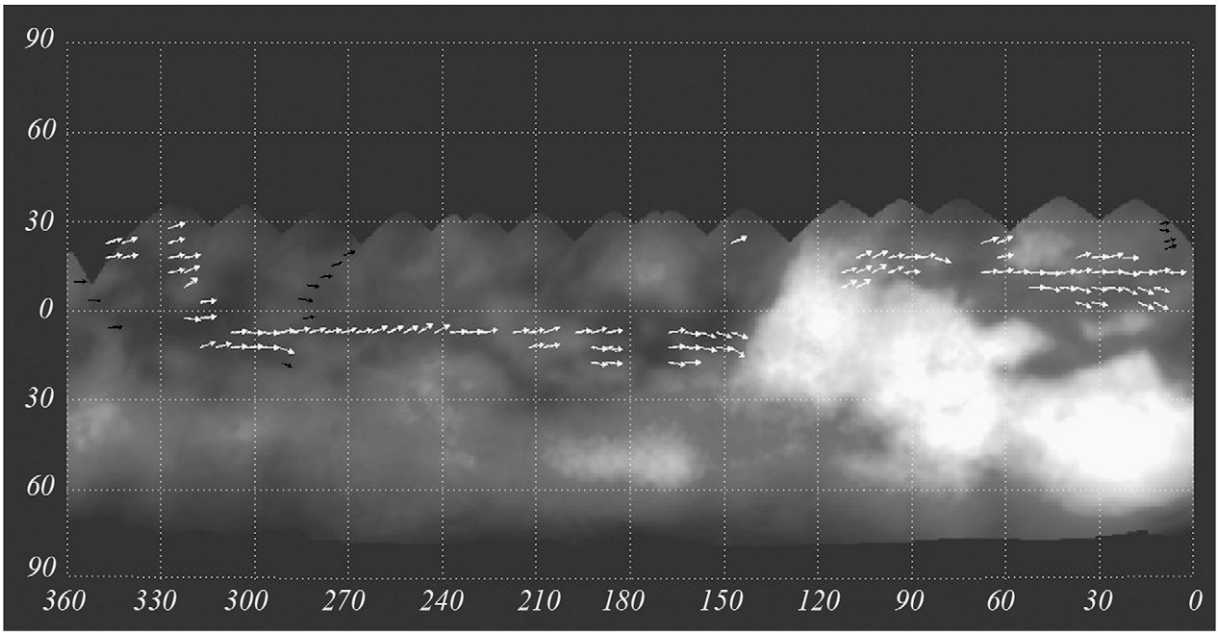


Fig. 10. Orientations of all dunes measured on Titan, binned in 5° × 5° latitude–longitude boxes. Histograms of dune azimuths were calculated for each box (dunes with length less than 5 km were discarded). Line orientations indicate mean dune orientations and arrowheads indicate hypothesized wind directions. Black vectors are preliminary measurements through T23. Image basemap courtesy of NASA Hubble Space Telescope.

(to the S), and is in agreement with wind models (e.g., Tokano and Neubauer, 2002), so this is a satisfying result. However, dunes north of the equator are deflected northward in several other locations, for example in the T19 swath (310°–330° W, 0°–10° N), in the T16 swath (140° W, 20° N), and in the middle of the T3 swath (60° W, 20° N). Dunes north of the equator may be deflected by other regions of high topography that are not yet revealed to radar, or their orientations may be used to help revise the revise the equatorward wind models.

Dunes in the T3, T13, and even T17 swaths show evidence of having been deflected by the massive Xanadu region (Fig. 10).

## 8. Global distribution and climate

The distribution of dunes across Titan's surface may give an indication of global, climatological processes, although certain assumptions must be made. Although dunes typically form on Earth in deserts, defined by their lack of a threshold yearly precipitation level, it is primarily sufficient sand supply and winds that control the presence of dunes. Thus, although increased precipitation levels, which would also elevate local humidities, may increase the "stickiness" of particles and inhibit their transport, we cannot readily relate the presence of dunes to conditions of low precipitation; although it will be discussed that other factors may contribute to a positive correlation. For example, because Titan's dune particles are likely mostly derived directly from atmospheric sources rather than surface erosion, the carriage of particles by meteoric liquids away from potential dune areas precludes dune formation in regions of high precipitation.

A crude estimate of the coverage of Titan's surface by dunes can be by calculating the area covered by the 5° × 5° latitude–longitude boxes (weighted by the cosine of latitude) and comparing it with the area covered by SAR. While nearly 5% of Titan's total surface has been observed to be covered in dunes, less than 30% of Titan's surface has been observed at appropriate resolution. In fact, of the terrain observed by SAR within 30° of the equator, ~40% of the area observed has some dunes (Figs. 4 and 11).

Given that there are many regions dark to near-IR that have dunes where there is Radar coverage, we expect that the coverage of dunes on Titan's surface greatly exceeds the already measured 5% and may approach 20% (Fig. 4). Longitudinal

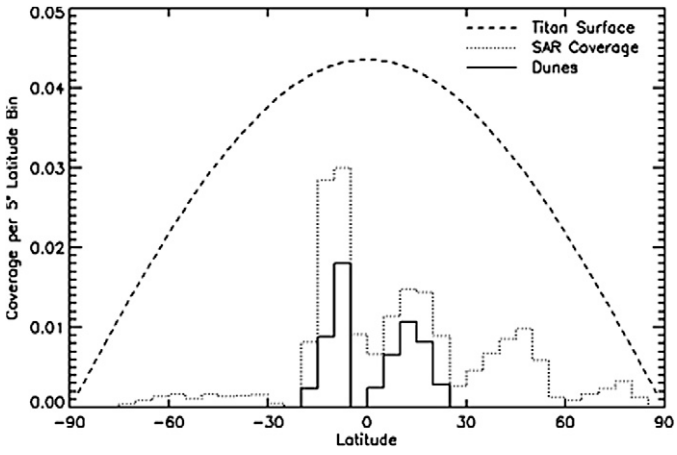


Fig. 11. Distribution of dunes and SAR coverage versus latitude, through the T18 swath. The dashed line indicates complete coverage (equal latitude bins cover smaller areas near the poles). The solid line shows the area covered by dunes, all within 30° of the equator in this plot. The peaks in the SAR coverage (dotted line) are left to right, T7, T8 + T13 covering a large part of Titan just south of the equator, T3 + T17, TA, T16 + T18. SAR passes T19–T30 would increase both overall SAR and dune coverage proportionally at latitudes less than 30°, and would increase the overall SAR coverage to 40–70% at latitudes greater than 60°.

dunes account for at least 95% of all dunes observed in Radar and near-IR images of Titan. In comparison, longitudinal dunes are also the most dominant dune form on Earth, covering on average 60–70% of Earth's sand seas (e.g., Lancaster, 1982). On Mars, longitudinal dunes have nearly the opposite proportion of all Mars dunes to that of Titan, there are very few (Lee and Thomas, 1995).

Although there are channels most likely carved by meteoric fluids (Lunine et al., 2008; Lorenz et al., 2007) interspersed with dunes, there is little evidence for currently present fluids at equatorial regions on Titan. An exception is in observations made at the Huygens landing site (10.3° S, 192.3° W), at which the ambient methane humidity was measured at the landing site to be ∼50% (Tomasko et al., 2005; Niemann et al., 2005). In addition, methane and ethane (both liquids) as well as other organics were detected in the material into which the Huygens probe landed—there was enough liquid present for the GCMS inlet to 'feel' cold due to the evaporation of this liquid (Lorenz et al., 2006). The presence of fluvial channels and rounded boulders at the landing site implies that rainfall and related processes shaped that particular spot on Titan's landscape (Tomasko et al., 2005; Collins, 2005; Barnes et al., 2007; see also Tokano et al., 2006). In addition to observations of fluvial channels and elevated humidities at the Huygens landing site, two presumed (they are visible only as dark streaks in the imagery to date) duneforms were observed about 20 km north of the landing site (Lunine et al., 2008).

This seeming paradox of dunes present where conditions of locally moderate humidities prevail is considered in the context of terrestrial desert distributions and cyclical processes. Deserts on Earth are found predominantly around latitudes of 25° N or S of the equator, due to the intersection of the dry, downwelling branch of the Hadley cell with the Earth's surface. On Titan, however, an asymmetric circulation regime prevails through most of the year, with upwelling at the summer pole and downwelling elsewhere (Hourdin et al., 1995). Thus, seasonally, the winter pole will have dry downwelling, as will low latitudes generally, except for a brief interval near equinox when a symmetric regime occurs before the pole-to-pole circulation resumes. This brief interval may allow for methane rainfall and accumulation in basins at equatorial regions. This is perhaps similar to the brief and strong summer storms in the U.S. desert southwest, which storms are also effective at carving channels that remain empty most of the year. More recent general circulation models (e.g., Rannou et al., 2006) predict low humidities at low latitudes, and damp conditions near the poles, consistent with the observation of lakes at Titan's north polar regions (Stofan et al., 2007) and of a large methane cloud encircling the northern polar regions (recent VIMS observations). Thus, the prevalence of dunes at low latitudes may be partly due to the generally but not strictly low humidity conditions at Titan's low latitudes. It should also be noted that sand seas on Earth can be relatively long-lived features compared with other aeolian landforms. It is in fact this longevity that may ultimately result in the longitudinal form (e.g., Tsoar, 1978). The process of accumulation of sediments prior to their organization and transportation can take thousands to tens of thousands of years (Lancaster, 1995). Thus, although the dunes themselves may be active and thus the youngest features on a surface, their presence may be more a reflection of past rather than current climatological conditions.

Several observations of Titan indicate that global processes may dominate over local processes in terms of geomorphological feature distribution. We outline these and then consider the effects of global processes on dune formation and distribution. The sediment source for dunes is considered to be dominantly atmospheric fallout (Wilson and Atreya, 2004), although there is likely contribution to dune sediments from erodable materials (Stofan et al., 2006). These surficially obtained materials are found in mountains, channel floors, and impact debris (Stofan et al., 2006; Lopes et al., 2007; Lorenz et al., 2007; Lunine et al., 2008). Assuming that dune-forming sediments are obtained evenly over the surface of Titan, dominantly from the atmosphere with minor contribution from erosion, then sediments must preferentially accumulate in one region (low latitudes) and be transported away from another (high latitudes and polar regions). Sediment sinks appear to be few and are perhaps concentrated near the poles in the form of lakes (Stofan et al., 2007), and observations of clouds, which may be related to methane rainfall, are found dominantly in polar regions (Griffith et al., 2006; recent VIMS observations). Titan's global, tidal, orbit-averaged wind pattern is equatorward of 45° latitude (Lorenz et al., 2006; Hourdin et al., 1995), and thus it is possible that the tidal winds have swept sediments towards low latitudes where the dunes are observed. The dune fields observed in T3, T16, T19, and T21 that are found at higher latitudes are small, with short, widely spaced dunes. This is consistent with a limited sand supply (e.g., Fitzsimmons, 2006) at those latitudes. Sediments have been pirated from these high-latitude regions to be carried to and trapped at low latitudes by equatorward winds, seasonally alternating winds (see Section 7), or topographic conditions, such as basins surrounded by higher topography.

All the directional indicators we have observed indicate a dominantly W-E wind trend. This trend is consistent with both the Huygens Doppler Wind and DISR tracking measurements (Folkner et al., 2005; Tomasko et al., 2005). The inferred eastward direction to the surface wind at all latitudes marked by the dunes contrasts with the GCM simulation for the 2004–2005 season by Tokano and Neubauer (2005), showing westward flow near the equator then, but more nearly resembles the approach they describe to the upcoming late winter. We have observed that dunes flow around, and are apparently deviated by, radar-bright and apparently high-standing areas, both on local and regional scales. Study with mesoscale models may help constrain how much influence topographic obstacles may have, and/or whether (for example) katabatic winds from bright or cool areas might similarly deviate regional winds around such areas.

With the companion discoveries of dunes at Titan's equatorial regions (Lorenz et al., 2006) and lakes at Titan's polar regions (Stofan et al., 2007) a picture of Titan's global weather and climate is beginning to emerge. It appears that methane rainfall occurs at Titan's poles (or perhaps its winter pole, currently the north pole; Stofan et al., 2006, 2007) while relatively

dry, desert-like conditions occur at the equator, where sediments have been shaped by winds into dunes (Lorenz et al., 2006). However, local variations on this global condition exist, both spatially and temporally. Thus, the major factors of generally low humidity, adequate sediment supply, sufficient winds, and absence of sediment trapping (in the form of rivers washing away sediments, basins containing fluids, etc.) must be considered together to explain the presence or absence of dunes on Titan. Since on Earth dunes can be found along many coastlines (including the chilly damp coasts of Western Europe) that are not associated with low humidity or lack of rainfall, the proximity of the Huygens channels to dunes is no more paradoxical than the existence of dunes on Noordwijk beach, the Netherlands. It only underscores that Titan is every bit as complex a world as is the Earth.

## 9. Conclusions

Many thousands of longitudinal dunes cover the surface of Titan, covering nearly 5% of its surface. These are in form and scale similar to longitudinal dunes found in many of Earth's deserts. Combined evidence indicates that these dunes form and evolve by dominant winds along the dune axes, with lesser, acutely-angled, off-axis winds or seasonal, obtusely angled winds. Based on observations and global compilations of dune orientations, these winds flow from W-E but are diverted around topographically high features such as mountain blocks or broad landforms such as Xanadu. Global winds may carry particulates from high latitudes to equatorial regions, where conditions are relatively drier. There, sediments accumulate in vast, shallow, dry basins where they are reworked into dunes, the whole process taking perhaps thousands to tens of thousands of years. Given the nearly invariant dune type on Titan regardless of sand supply and topographic interactions, winds on Titan must have a consistent direction, strength, and persistence over time to create and maintain the observed duneforms.

## Acknowledgments

The authors acknowledge the excellent performance of and rich data returned by the Cassini spacecraft. We thank the JPL engineers for their painstaking efforts in achieving and maintaining operational smoothness. We also thank reviewers Devon Burr and Mary Bourke for their careful, candid, and clarifying reviews of this work, and Tom Farr, Zibi Turtle, and Jason Barnes for their extremely helpful comments. Research was done primarily under the support of the NASA Cassini program, and at the University of Arizona and Brigham Young University.

## References

Bagnold, R., 1942. Physics of Wind-blown Sand and Desert Dunes. W. Morrow and Co., New York, 265 pp.

Barnes, J.W., Brown, R.H., Radebaugh, J., Buratti, B.J., Sotin, C., Le Mouelic, S., Rodriguez, S., Turtle, E.P., Perry, J., Clark, R., Baines, K.H., Nicholson, P.D., 2006. Cassini observations of flow-like features in western Tui Regio, Titan. Geophys. Res. Lett. 33, doi:10.1029/2006GL026843. L16204.

Barnes, J.W., Radebaugh, J., Brown, R.H., Wall, S., Soderblom, L., Lunine, J., Burr, D., Sotin, C., Le Mouélic, S., Rodriguez, S., Buratti, B.J., Clark, R., Baines, K.H., Jaumann, R., Nicholson, P.D., Kirk, R.L., Lopes, R., Lorenz, R.D., Mitchell, K., Wood, C.A., and the Cassini Radar Team, 2007. Near-infrared spectral mapping of Titan's mountains and channels. J. Geophys. Res. 112, doi:10.1029/2007JE002932. E11006.

Bird, M.K., Allison, M., Asmar, S.W., Atkinson, D.H., Avruch, I.M., Dutta-Roy, R.R., Dzierma, Y., Edenhofer, P., Folkner, W.M., Gurvits, L.I., Johnson, D.V., Plettemeier, D., Pogrebenko, S.V., Preston, R.A., Tyler, G.L., 2005. The vertical profile of winds on Titan. Nature 438, 800–802.

Blandford, W.T., 1877. Geological notes on the great desert between Sind and Rajputana. Geol. Surv. India Records 10, 10–21.

Blumberg, D.G., Greeley, R., 1996. A comparison of general circulation model predictions to sand drift and dune orientations. J. Climate 9, 3248–3259.

Boubin, G.M., Reffet, E.G., Lunine, J.I., Radebaugh, J., Lopes, R.M., and the Cassini Radar Team, 2005. Mapping and characterization of "cat scratches" on Titan. Bull. Am. Astron. Soc. 37. Abstract 46.04.

Bourke, M.C., Bullard, J.E., Barnouin-Jha, O.S., 2004. Aeolian sediment transport pathways and aerodynamics at troughs on Mars. J. Geophys. Res. 109, doi:10.1029/2003JE002155.

Bowen, A.J., Lindley, D., 1977. A wind tunnel investigation of the wind speed and turbulence characteristics close to the ground over various escarpment shapes. Bound. Layer Meteorol. 12, 259–271.

Callahan, P.S., Hensley, S., Gim, Y., Johnson, W.T., Lorenz, R.D., Alberti, G., Orosei, R., Seu, R., Franceschetti, G., Paillou, P., Paganelli, F., Wall, S., West, R.D., 2006. Information on Titan's surface from Cassini Radar Altimeter waveforms. Eos (Fall Suppl.) 87 (52). P13A-0165.

Collins, G.C., 2005. Relative rates of fluvial bedrock incision on Titan and Earth. Geophys. Res. Lett. 32, doi:10.1029/2005GL024551. L22202.

Cooke, R.U., Warren, A., Goudie, A., 1993. Desert Geomorphology. UCL Press Limited, London.

Dobrovolskis, A.R., 1993. Atmospheric tides on Venus. IV. Topographic winds and sediment transport. Icarus 103, 276–289.

Elachi, C., Wall, S., Allison, M., Anderson, Y., Boehmer, R., Callahan, P., Encrenaz, P., Flameni, E., Francescetti, G., Gim, Y., Hamilton, G., Hensley, S., Janssen, M., Johnson, W., Kelleher, K., Kirk, R., Lopes, R., Lorenz, R., Lunine, J., Muhleman, D., Ostro, S., Paganelli, F., Picardi, G., Posa, F., Roth, L., Seu, R., Shaffer, S., Soderblom, L., Stiles, B., Stofan, E., Vetrella, S., West, R., Wood, C., Wye, L., Zebker, H., 2005. Cassini Radar views the surface of Titan. Science 308, 970–974.

Elachi, C., Wall, S., Janssen, M., Stofan, E., Lopes, R., Kirk, R., Lorenz, R., Lunine, J., Paganelli, F., Soderblom, L., Wood, C., Wye, L., Zebker, H., Anderson, Y., Ostro, S., Allison, M., Boehmer, R., Callahan, P., Encrenaz, P., Flameni, E., Francescetti, G., Gim, Y., Hamilton, G., Hensley, S., Johnson, W., Kelleher, K., Muhleman, D., Picardi, G., Posa, F., Roth, L., Seu, R., Shaffer, S., Stiles, B., Vetrella, S., West, R., 2006. Titan Radar Mapper observations from Cassini's T3 fly-by. Nature 441, 709–713.

Fitzsimmons, K.E., 2006. Regional landform patterns in the Strzelecki Desert dunefield: Dune migration and mobility at large scales. In: Fitzpatrick, R.W., Shand, P. (Eds.), Proceedings of the CRC LEME Regolith Symposium. Cooperative Research Centre for Landscape Environments and Mineral Exploration, Perth, Western Australia, pp. 95–99.

Folk, R., 1971. Genesis of longitudinal and oghurd dunes elucidated by rolling upon grease. Geol. Soc. Am. Bull. 82, 3461–3468.

Folkner, W.M., Asmar, S.W., Border, J.S., Franklin, G.W., Finley, S.G., Gorelik, J., Johnston, D.V., Kerzhanovich, V.V., Lowe, S.T., Preston, R.A., Bird, M.K., Dutta-Roy, R., Allison, M., Atkinson, D.H., Edenhofer, P., Plettemeier, D., Tyler, G.L., 2005. Winds on Titan from ground-based tracking of the Huygens probe. J. Geophys. Res. 111, doi:10.1029/2005JE002649.

Fryberger, S.G., Dean, G., 1979. Dune forms and wind regime. In: McKee, E.D. (Ed.), A Study of Global Sand Seas. In: U.S. Geol. Surv. Prof. Pap., vol. 1052, pp. 137–169.

Fryberger, S.G., Ahlbrandt, T.S., 1979. Mechanisms for the formation of aeolian sand seas. Z. Geomorphol. 23, 440–460.

Greeley, R., Lancaster, N., Lee, S., Thomas, P., 1992. Martian aeolian processes, sediments and features. In: Keiffer, H.H., Jakosky, B.M., Snyder, C.W., Matthews, M.S. (Eds.), Mars. University of Arizona Press, Tucson, AZ, pp. 730–766.

Griffith, C.A., Penteado, P., Rannou, P., Brown, R., Boudon, V., Baines, K.H., Clark, R., Drossart, P., Buratti, B., Nicholson, P., McKay, C.P., Coustenis, A., Negrao, A., Jaumann, R., 2006. Evidence for a polar ethane cloud on Titan. Science 313, 1620–1622.

Hourdin, F., Talagrand, O., Sadourny, R., Courtin, R., Gautier, D., McKay, C.P., 1995. Numerical simulation of the general circulation of the atmosphere of Titan. Icarus 117, 358–374.

Kirk, R.L., Callahan, P., Seu, R., Lorenz, R.D., Paganelli, F., Lopes, R.M., Elachi, C., and the Cassini Radar Team, 2005. Radar reveals Titan topography. Lunar Planet. Sci. XXXVI. Abstract 2227.

Lancaster, N., 1980. The formation of seif dunes from barchans—Supporting evidence for Bagnold's hypothesis from the Namib Desert. Z. Geomorphol. 24, 160–167.

Lancaster, N., 1982. Linear dunes. Prog. Phys. Geog. 6, 476–504.

Lancaster, N., 1989. The Namib Sand Sea: Dune Forms, Processes, and Sediments. A.A. Balkema, Rotterdam, 200 pp.

Lancaster, N., 1995. The Geomorphology of Desert Dunes. Routeledge, London/New York, 290 pp.

Lee, P., Thomas, P.C., 1995. Longitudinal dunes on Mars: Relation to current wind regimes. J. Geophys. Res. 100, 5381–5395.

Lopes, R.M., Stofan, E.R., Mitchell, K.L., Wall, S.D., Wood, C.A., Lorenz, R.D., Paganelli, F., Lunine, J., Radebaugh, J., and the Cassini Radar Team, 2006. Titan's surface: Distribution of endogenic and exogenic processes from Cassini Radar data. Bull. Am. Astron. Soc. 38. Abstract 52.02.

Lopes, R.M.C., Mitchell, K.L., Stofan, E.R., Lunine, J.I., Lorenz, R., Paganelli, F., Kirk, R.L., Wood, C.A., Wall, S.D., Robshaw, L.E., Fortes, A.D., Neish, C.D., Radebaugh, J., Reffet, E., Ostro, S.J., Elachi, C., Allison, M.D., Anderson, Y., Boehmer, R., Boubin, G., Callahan, P., Encrenaz, P., Flamini, E., Francescetti, G., Gim, Y., Hamilton, G., Hensley, S., Janssen, M.A., Johnson, W.T.K., Kelleher, K., Muhleman, D.O., Ori, G., Orosei, R., Picardi, G., Posa, F., Roth, L.E., Seu, R., Shaffer, S., Soderblom, L.A., Stiles, B., Vetrella, S., West, R.D., Wye, L., Zebker, H.A., 2007. Cryovolcanic features on Titan's surface as revealed by the Cassini Titan Radar Mapper. Icarus 186, 395–412.

Lorenz, R.D., Wall, S., Radebaugh, J., Boubin, G., Reffet, E., Janssen, M., Stofan, E., Lopes, R., Kirk, R., Elachi, C., Lunine, J., Paganelli, F., Soderblom, L., Wood, C., Wye, L., Zebker, H., Anderson, Y., Ostro, S., Allison, M., Boehmer, R., Callahan, P., Encrenaz, P., Ori, G.G., Francescetti, G., Gim, Y., Hamilton, G., Hensley, S., Johnson, W., Kelleher, K., Mitchell, K., Muhleman, D., Picardi, G., Posa, F., Roth, L., Seu, R., Shaffer, S., Stiles, B., Vetrella, S., Flamini, E., West, R., 2006. The sand seas of Titan: Cassini Radar observations of longitudinal dunes. Science 312, 724–727.

Lorenz, R.D., Lopes, R.M., Paganelli, F., Lunine, J.I., Kirk, R.L., Soderblom, L.A., Stofan, E.R., Ori, G., Myers, M., Miyamoto, H., Stiles, B., Wall, S.D., Wood C.A., and the Cassini Radar Team, 2007. Fluvial channels on Titan: Meteorological paradigm and Cassini Radar observations. Planet. Space Sci., submitted for publication.

Lunine, J.I., Elachi, C., Wall, S.D., Janssen, M.A., Allison, M.D., Anderson, Y., Boehmer, R., Callahan, P., Encrenaz, P., Flamini, E., Franceschetti, G., Gim, Y., Hamilton, G., Hensley, S., Johnson, W.T.K., Kelleher, K., Kirk, R.L., Lopes, R.M., Lorenz, R., Muhleman, D.O., Orosei, R., Ostro, S.J., Paganelli, F., Paillou, P., Picardi, G., Posa, F., Radebaugh, J., Roth, L.E., Seu, R., Shaffer, S., Soderblom, L.A., Stiles, B., Stofan, E.R., Vetrella, S., West, R., Wood, C.A., Wye, L., Zebker, H., Alberti, G., Karkoschka, E., Rizk, B., McFarlane, E., See, C., Kazeminejad, B., 2008. Titan's diverse landscape as evidenced by Cassini RADAR's third and fourth looks at Titan. Icarus, in press.

Mainguet, M., Callot, Y., 1978. L'erg de Fachi–Bilma (Tchad–Niger). Mem. Doc. CNRS 18, 178.

McKee, E.D., 1982. Sedimentary structures in dunes of the Namib Desert, South West Africa. Geol. Soc. Am. Spec. Pap. 188, 1–64.

McLean, S.R., Nelson, J.M., Wolfe, S.R., 1994. Turbulence structure over two-dimensional bed forms: Implications for sediment transport. J. Geophys. Res. 99, 12729–12747.

Niemann, H.B., Atreya, S.K., Bauer, S.J., Carignan, G.R., Demick, J.E., Frost, R.L., Gautier, D., Haberman, J.A., Harpold, D.N., Hunten, D.M., Israel, G., Lunine, J.I., Kasprzak, W.T., Owen, T.C., Paulkovich, M., Raulin, F., Raaen, E., Way, S.H., 2005. The abundances of constituents of Titan's atmosphere from the GCMS instrument on the Huygens probe. Nature 438, 779–784.

Paganelli, F., Callahan, P., Hensley, S., Lorenz, R., Lunine, J., Kirk, R., Stiles, B., Janssen, M., Lopes, R., Stofan, E., Wall, S., Paillou, P., and the Cassini Radar Team, 2006. A different look at Titan's dunes. Bull. Am. Astron. Soc. 38. Abstract 56.08.

Paganelli, F., Janssen, M.A., Stiles, B., West, R., Lorenz, R.D., Lunine, J.I., Lopes, R.M., Stofan, E., Kirk, R.L., Roth, L., Wall, S.D., Elachi, C., and the Cassini Radar Team, 2007a. Titan's surface from the Cassini Radar SAR and high-resolution radiometry data of the first five flybys. Icarus 191, 211–222.

Paganelli, F., Janssen, M.A., Lopes, R.M., Stofan, E., Wall, S.D., Lorenz, R.D., Lunine, J.I., Kirk, R.L., Roth, L., Elachi, C., and the Cassini Radar Team, 2007b. Titan's surface from the Cassini RADAR radiometry data during SAR mode. Planet. Space Sci. Special Issue EGU 2006, doi:10.1016/j.physletb.2003.10.071.

Porco, C.C., Baker, E., Barbara, J., Beurle, K., Brahic, A., Burns, J.A., Charnoz, S., Cooper, N., Dawson, D.D., Del Genio, A.D., Denk, T., Dones, L., Dyudina, U., Evans, M.W., Fussner, S., Giese, B., Grazier, K., Helfenstein, P., Ingersoll, A.P., Jacobson, R.A., Johnson, T.V., McEwen, A., Murray, C.D., Neukum, G., Owen, W.M., Perry, J., Roatsch, T., Spitale, J., Squyres, S., Thomas, P., Tiscareno, M., Turtle, E.P., Vasavada, A.R., Veverka, J., Wagner, R., West, R., 2005. Imaging of Titan from the Cassini spacecraft. Nature 434, 159–168.

Radebaugh, J., Lorenz, R., Lunine, J., Wall, S., Boubin, G., Reffet, E., Kirk, R., Lopes, R., Stofan, E., Soderblom, L., Allison, M., 2006. Longitudinal dunes on Titan as indicators of regional and local winds. Eos (Fall Suppl.) 87 (52). P12A-03.

Radebaugh, J., Lorenz, R.D., Kirk, R.L., Lunine, J.I., Stofan, E.R., Lopes, R.M.C., Wall, S.D., and the Cassini Radar Team, 2007. Mountains on Titan observed by Cassini Radar. Icarus 192, 77–91.

Rannou, P., Montmessin, F., Hourdin, F., Lebonnois, S., 2006. The latitudinal distribution of clouds on Titan. Science 311, 201–205.

Rubin, D.M., Ikeda, H., 1990. Flume experiments on the alignment of transverse, oblique and longitudinal dunes in directionally varying flows. Sedimentology 37, 673–684.

Saunders, R.S., Dobrovolskis, A.R., Greeley, R., Wall, S.D., 1990. Large-scale patterns of eolian sediment transport on Venus: Predictions for Magellan. Geophys. Res. Lett. 17, 1365–1368.

Soderblom, L., Anderson, J., Baines, K., Barnes, J., Barrett, J., Brown, R., Buratti, B., Clark, R., Cruikshank, D., Elachi, C., Janssen, M., Jaumann, R., Kirk, R., Karkoschka, E., Lemouelic, S., Lopes, R., Lorenz, R., Lunine, J., McCord, T., Nicholson, P., Radebaugh, J., Rizk, B., Sotin, C., Stofan, E., Sucharski, T., Tomasko, M., Wall, S., 2007. Correlations between Cassini VIMS spectra and RADAR SAR images: Implications for Titan's surface composition and the character of the Huygens Probe landing site. Planet. Space Sci. 55, 2025–2036.

Stofan, E.R., Lunine, J.I., Lopes, R., Paganelli, F., Lorenz, R.D., Wood, C.A., Kirk, R., Wall, S., Elachi, C., Soderblom, L.A., Ostro, S., Janssen, M., Radebaugh, J., Wye, L., Zebker, H., Anderson, Y., Allison, M., Boehmer, R., Callahan, P., Encrenaz, P., Flamini, E., Francescetti, G., Gim, Y., Hamilton, G., Hensley, S., Johnson, W.T.K., Kelleher, K., Muhleman, D., Picardi, G., Posa, F., Roth, L., Seu, R., Shaffer, S., Stiles, B., Vetrella, S., West, R., 2006. Mapping of Titan: Results from the first two Titan Radar passes. Icarus 185, 443–456.

Stofan, E.R., Elachi, C., Lunine, J.I., Lorenz, R.D., Stiles, B., Mitchell, K.L., Ostro, S., Soderblom, L., Wood, C., Zebker, H., Wall, S., Janssen, M., Kirk, R., Lopes, R., Paganelli, F., Radebaugh, J., Wye, L., Anderson, Y., Allison, M., Boehmer, R., Callahan, P., Encrenaz, P., Flamini, E., Francescetti, G., Gim, Y., Hamilton, G., Hensley, S., Johnson, W.T.K., Kelleher, K., Muhleman, D., Paillou, P., Picardi, G., Posa, F., Roth, L., Seu, R., Shaffer, S., Vetrella, S., West, R., 2007. The lakes of Titan. Nature 445, 61–64.

Tokano, T., Lorenz, R.D., 2006. GCM simulation of balloon trajectories on Titan. Planet. Space Sci. 54, 685–694.

Tokano, T., Neubauer, F.M., 2002. Tidal winds on Titan caused by Saturn. Icarus 158, 499–515.

Tokano, T., Neubauer, F.M., 2005. Wind-induced seasonal angular momentum exchange at Titan's surface and its influence on Titan's length-of-day. Geophys. Res. Lett. 32, doi:10.1029/2005GL024456. L24203.

Tokano, T., McKay, C.P., Neubauer, F.M., Atreya, S.K., Ferri, F., Fulchignoni, M., Niemann, H.B., 2006. Methane drizzle on Titan. Nature 442, 432–435.

Tomasko, M.G., Archinal, B., Becker, T., Bézard, B., Bushroe, M., Combes, M., Cook, D., Coustenis, A., de Bergh, C., Dafoe, L.E., Doose, L., Douté, S., Eibl, A., Engel, S., Gliem, F., Grieger, B., Holso, K., Howington-Kraus, E., Karkoschka, E., Keller, H.U., Kirk, R., Kramm, R., Küppers, M., Lanagan, P., Lellouch, E., Lemmon, M., Lunine, J., McFarlane, E., Moores, J., Prout, G.M., Rizk, B., Rosiek, M., Rueffer, P., Schröder, S.E., Schmitt, B., See, C., Smith, P., Soderblom, L., Thomas, N., West, R., 2005. Rain, winds and haze during the Huygens probe's descent to Titan's surface. Nature 438, 765–778.

Townsend, A.A., 1976. The Structure of Turbulent Shear Flow, second ed. Cambridge University Press, Cambridge, 429 pp.

Tsoar, H., 1978. The dynamics of longitudinal dunes. Final technical report to the U.S. Army European Research Office. U.S. Army European Research Office, London.

Tsoar, H., 1983. Dynamic processes acting on a longitudinal (seif) dune. Sedimentology 30, 567–578.

Turtle, E.P., Perry, J., McEwen, A.S., West, R.A., Fussner, S., 2007. Titan's surface as revealed by Cassini's Imaging Science Subsystem. Lunar Planet. Sci. XXXVIII. Abstract 2322.

Weitz, C.M., Plaut, J.J., Greeley, R., Saunders, R.S., 1994. Dunes and microdunes on Venus: Why were so few found in the Magellan data? Icarus 112, 282–295.

Wilson, I.G., 1971. Desert sandflow basins and a model for the development of ergs. Geogr. J. 137, 180–199.

Wilson, E.H., Atreya, S.K., 2004. Current state of modeling the photochemistry of Titan's mutually dependent atmosphere and ionosphere. J. Geophys. Res. 109, doi:10.1029/2003JE002181. E06002.